THE JOURNAL OF BIOLOGICAL CHEMISTRY VOL. 283, NO. 12, pp. 7790–7803, March 21, 2008

BIM and tBID Are Not Mechanistically Equivalent When Assisting BAX to Permeabilize Bilayer Membranes*[S]

Received for publication, October 25, 2007, and in revised form, January 11, 2008 Published, JBC Papers in Press, January 14, 2008, DOI 10.1074/jbc.M708814200

Oihana Terrones[‡1], Aitor Etxebarria[‡1], Ane Landajuela[‡], Olatz Landeta[‡], Bruno Antonsson[§], and Gorka Basañez[‡2]

From the [‡]Unidad de Biofísica (Centro Mixto Consejo Superior de Investigaciones Cientificas, Universidad del Pais Vasco/Euskal Herriko Unibertsitatea), Universidad del Pais Vasco/Euskal Herriko Unibertsitatea, P. O. Box 644, 48080 Bilbao, Spain and [§]Merck Serono International S. A., 9 chemin des Mines, 1202 Geneva, Switzerland

BIM and tBID are two BCL-2 homology 3 (BH3)-only proteins with a particularly strong capacity to trigger BAX-driven mitochondrial outer membrane permeabilization, a crucial event in mammalian apoptosis. However, the means whereby BIM and tBID fulfill this task is controversial. Here, we used a reconstituted liposomal system bearing physiological relevance to explore systematically how the BAX-permeabilizing function is influenced by interactions of BIM/BID-derived proteins and BH3 motifs with multidomain BCL-2 family members and with membrane lipids. We found that nanomolar dosing of BIM proteins sufficed to reverse completely the inhibition of BAX permeabilizing activity exerted by all antiapoptotic proteins tested (BCL-2, BCL-X_L, BCL-W, MCL-1, and A1). This effect was reproducible by a peptide representing the BH3 motif of BIM, whereas an equivalent BID BH3 peptide was less potent and more selective, reversing antiapoptotic inhibition. On the other hand, in the absence of BCL-2-type proteins, BIM proteins and the BIM BH3 peptide were inefficient, directly triggering the BAX-permeabilizing function. In contrast, tBID alone potently assisted BAX to permeabilize membranes at least in part by producing a structural distortion in the lipid bilayer via BH3-independent interaction of tBID with cardiolipin. Together, these results support the notion that BIM and tBID follow different strategies to trigger BAX-driven mitochondrial outer membrane permeabilization with strong potency.

One of the decisive events in mammalian apoptosis is the MOMP[3] resulting in release of multiple apoptogenic factors, including cytochrome *c*, from the intermembrane space into the cytosol (1). The BCL-2 protein family has emerged as the master regulator of this crucial step in the intracellular apoptotic cascade (Refs. 1–3 but see Ref. 4). Based on sequence homology and functional criteria, this family can be divided into three main subclasses (2). One subclass includes the antiapoptotic proteins BCL-2, BCL-W, BCL-X_L, MCL-1, BFL-1/A1, and BCL-B, all of which possess four BCL-2 homology domains (BH1–4) and inhibit MOMP. A second subclass is represented by proapoptotic BAX and BAK, which contain BH1–3 domains and are directly responsible for MOMP. Finally, members of the more distantly related BH3-only subclass (tBID, BIM, PUMA, BAD, NOXA, HRK, BIK, and BMF) display sequence homology only within the third BH domain and promote apoptosis by triggering BAX-driven MOMP.

It is agreed that BAX-type proteins exist in an inactive state in healthy cells and that BH3-only proteins funnel multiple apoptotic signals to activate the permeabilizing function of BAX/BAK. However, the means whereby BH3-only members perform this task is a subject of current debate (2, 3, 5, 6). BIM and tBID are two well known BH3-only members with a particularly high potency for triggering BAX-driven MOMP and apoptotic cell death. Two main models evolved in the last few years to explain the highly lethal activity of BIM and tBID. On the one hand, the so-called "displacement model" postulates that BIM and tBID physically interact with all five BCL-2-type proteins to competitively displace BAX/BAK, thereby indirectly activating the permeabilizing function of BAX-type proteins (7). Indeed, multiple binding assays (7–11) and structural analysis (12–15) sustain the notion that BH1-BH3 domains define the entry of an elongated hydrophobic pocket on the surface of BCL-2-type proteins, which can accept the BH3 domain of proapoptotic partners corresponding to an amphipathic α-helix. However, although it is firmly established that BIM binds the whole panel of antiapoptotic proteins with low nanomolar affinity constants via its BH3 domain, evidence indicating that tBID engages the complete set of BCL-2-type proteins with strong affinity is tenuous. Alternatively, according to the "direct model" the potent proapoptotic activity of BIM and tBID originates from the exclusive capacity of their BH3 domains to directly bind to and activate the permeabilizing function of BAX/BAK (9–11, 16–18). In support of this view, *in vitro* studies demonstrated that hydrocarbon-stapled BIM/BID BH3 peptides can interact with BAX with nanomolar affinity constants (16). Yet, it remains to be clarified how closely the behavior of such chemically modified peptides reflects that of parent proteins as well as the exact molecular pathway by which the BIM/BID BH3-BAX interaction leads to MOMP.

* This work was supported in part by Ministerio de Ciencia y Tecnologia Grant BFU2005-06095. The costs of publication of this article were defrayed in part by the payment of page charges. This article must therefore be hereby marked "*advertisement*" in accordance with 18 U.S.C. Section 1734 solely to indicate this fact.

[S] The on-line version of this article (available at http://www.jbc.org) contains supplemental Table 1 and Figs. 1–6.

[1] Recipients of predoctoral fellowships from the Basque Government.

[2] To whom correspondence should be addressed: Unidad de Biofísica (CSIC-UPV/EHU), Barrio Sarriena s/n, Leioa 48940, Spain. Tel.: 34-94-6013355; Fax: 34-94-6013360; E-mail: gbzbaasg@lg.ehu.es.

[3] The abbreviations used are: MOMP, mitochondrial outer membrane (MOM) permeabilization; FD70, fluorescein isothiocyanate-labeled dextrans of 70 kDa; PC, phosphatidylcholine; PE, phosphatidylethanolamine; PI, phosphatidylinositol; CL, cardiolipin; DOGS-NTA-Ni, 1,2,-dioleoyl-sn-glycero-3-{[*N*-5-amino-1-carboxylpentyl)-iminodiacetic acid]succinyl}; LUV, large unilamellar vesicles; BH, BCL-2 homology.

Albeit for completely different reasons, the aforementioned two models share the view that BIM and tBID are mechanistically equivalent, triggering the functional activation of BAX. However, evidence exists contradicting this notion. First, pioneering work by Martinou and co-workers (19) showed that recombinant BIM_L and tBID did not elicit the release of cytochrome *c* from isolated mitochondria in the same manner. In addition, structural studies revealed that tBID displays a helical globular fold similar to that found in multidomain BCL-2 family members and certain pore-forming toxins, whereas BIM is an intrinsically disordered protein (2, 12, 20). It has also been established that unlike BIM (21), tBID alone can exert deleterious effects on the viability of yeast cells (22) and that tBID (23, 24), but not BIM (21), can cooperate with BAX via a BH3-independent mechanism to kill yeast cells, which are devoid of BCL-2 family proteins. Last, multiple reports indicate that interaction with the mitochondrion-specific lipid CL plays a key role in the pro-apoptotic actions of tBID (23–29), whereas no evidence has been gathered so far implicating CL in BIM function during apoptosis. Thus, taken together, these studies leave open the question as to whether BIM and tBID trigger the functional activation of BAX-type proteins through the same mechanism or whether their mode of action is manifold.

Studies of the mode of BCL-2 protein action with intact cells are difficult to interpret at the molecular level mainly due to the complexity of the apoptotic network. This and other laboratories have successfully reconstituted important aspects of BCL-2 protein function in purely lipidic vesicular systems (10, 16, 17, 30–40). Here, we have attempted to elucidate the apoptotic mode of BIM and tBID action by thoroughly characterizing the effects of various recombinant BCL-2 family proteins and selected BH3 peptides on a reconstituted liposomal system bearing physiological significance. The results obtained indicate that BIM and tBID use different molecular mechanisms to effectively trigger the permeabilizing function of BAX.

EXPERIMENTAL PROCEDURES

Materials—KCl, HEPES, EDTA, $MgCl_2$, dodecyl octaethylene glycol monoether ($C_{12}E_8$), melittin, *Staphylococcus aureus* α-toxin (α-toxin), tetanolysin, and fluorescein isothiocyanate-labeled dextrans of 70 kDa (FD70) were obtained from Sigma. Egg phosphatidylcholine (PC), egg phosphatidylethanolamine (PE), liver phosphatidylinositol (PI), heart cardiolipin (CL), and 1,2,-dioleoyl-sn-glycero-3-{[N-5-amino-1-carboxylpentyl)-iminodiacetic acid]succinyl} (nickel salt) (DOGS-NTA-Ni) were purchased from Avanti Polar Lipids, Inc. (Alabaster, AL). Disuccinimidyl suberate was purchased from Molecular Probes (Eugene, OR).

Protein Production—All proteins, including BAX, were purified from soluble fractions of bacterial extracts obtained in the absence of detergents and were >90% pure electrophoretically (supplemental Fig. 1). Recombinant His_6-tagged full-length monomeric human BAX (BAX) (36), His_6-tagged human monomeric BAX lacking the C-terminal 20 amino acids (BAXΔC) (35), His_6-tagged murine BID (BID) and its mutants 97A98A and 94A (41), His_6-tagged human BIM_{EL} lacking the C-terminal 22 amino acids (BIM_{EL}ΔC) (42), and His_6-tagged human BCL-2 lacking the C-terminal 24 amino acids (BCL-2ΔC) (41) were obtained as previously described. To obtain caspase-8-cleaved BID (tBID), granzyme B-cleaved BID (t_gBID), and calpain-cleaved BID ($t_{cal}BID$), indicated proteases were incubated with BID in appropriate buffers at 1/100 (mol/mol) ratio for 1 h at 37 °C. Recombinant murine BIM_L (BIM_LΔC) was either (i) purchased from R&D systems with a His_6 tag and lacking the C-terminal 20 amino acids (assays corresponding to results shown in Figs. 2, *B* and *C*) or (ii) obtained from bacterial expression with a glutathione *S*-transferase tag and lacking the C-terminal 27 amino acids (all other assays). Recombinant His_6-tagged human BCL-W lacking the C-terminal 29 amino acids (BCL-WΔC), human glutathione *S*-transferase (GST)-tagged BCL-X_L lacking the C-terminal 24 amino acids (BCL-X_LΔC), mouse GST-tagged A1 lacking the C-terminal 20 amino acids (A1ΔC), and mouse GST-tagged MCL-1 lacking the N-terminal 151 amino acids and the C-terminal 23 amino acids (MCL-1ΔC) were obtained as described previously (8, 43) and purified by affinity chromatography followed by Superdex 200 size-exclusion chromatography. High performance liquid chromatography-purified 21-mer BIM/BID BH3 peptides and the 29-mer BID BH3 peptide were obtained from Abgent (San Diego, CA). Peptide identity was confirmed by electrospray mass spectroscopy.

Cytochrome c Release Assays—Mitochondria were isolated from livers of male Harlan Sprague-Dawley rats as described previously (30) and used within 3 h. Isolated mitochondria (500 μg of protein/ml) were incubated for 20 min at 37 °C with recombinant proteins in 50 μl of 125 mM KCl, 5 mM KH_2PO_4, 25 μM EGTA, 5 mM succinate, 5 μM rotenone, and 10 mM HEPES-KOH, pH 7.2. Reaction mixtures were centrifuged at 14,000 × *g* for 10 min to isolate the pellet and supernatant fractions, and cytochrome *c* contents were determined quantitatively using a colorimetric enzyme-linked immunosorbent assay (R&D Systems). The percentage of cytochrome *c* released into the supernatant (% cytochrome *c*) was calculated according to the equation, % cytochrome c = ([cytochrome c_{sup} − cytochrome c_{backgr}]/[cytochrome c_{total} − cytochrome c_{backgr})] × 100, where background release represents cytochrome *c* detected in the supernatant of buffer-treated samples, and total release represents cytochrome *c* measured in Triton X-100-treated samples. Absorbance measurements were carried on a Biotek Synergy HT fluorescence microplate reader (Winooski, VT).

Liposome Preparation—Unless otherwise stated, liposomes were prepared with lipid composition resembling that of mitochondrial outer membrane (MOM) contact sites ((40 PC/35 PE/10 PI/15 CL (mol/mol)] (MOM-mimetic liposomes)). Organic solvents were removed by evaporation under a N_2 stream followed by incubation under vacuum for 2 h. Dry lipid films were resuspended by vigorous vortexing in 100 mM KCl, 10 mM Hepes, pH 7.0, 0.1 mM EDTA (KHE buffer) resulting in the generation of multilamellar vesicles. For assays of vesicle contents, release KHE buffer was supplemented with 100 mg/ml FD70. Multilamellar vesicles were then subjected to five freeze/thaw cycles. These frozen/thawed liposomes were used in assays of direct protein binding assays and lipid morphological and structural studies. Large unilamellar vesicles (LUV) were produced by extrusion through two polycarbonate mem-

branes of 0.2-μm pore size (Nucleopore, San Diego, CA). Untrapped FD70 was removed by gel filtration in Sephacryl S-500 HR columns.

Fluorimetric Measurements of Vesicular Contents Release—Release of LUV-encapsulated FD70 was monitored in an SLM-2 Aminco-Bowman luminescence spectrometer (Spectronic Instruments, Rochester, NY) in a thermostatted 1-cm path length cuvette with constant stirring at 37 °C (V_{final} = 1 ml). λ_{ex} was 490, and λ_{em} was 530 nm (slits, 4 nm). A 515-nm cut-off filter was placed between the sample and the emission monochromator to avoid scattering interferences. The extent of marker release was quantified on a percentage basis according to the equation $(F_t - F_0/F_{100} - F_0) = 100$ where F_t is the measured fluorescence of protein-treated LUV at time t, F_0 is the initial fluorescence of the LUV suspension before protein addition, and F_{100} is the fluorescence value after complete disruption of LUV by addition of $C_{12}E_8$ (final concentration, 0.5 mM). Lipid concentration was 50 μM.

Binding of Proteins to MOM-mimetic Liposomes—To examine the binding of different BCL-2- family members to liposomes in a direct manner, proteins and freeze/thawed MOM-mimetic liposomes (500 μM lipid) were incubated in KHE buffer for 20 min at 37 °C (V_{final} = 100 μl). The mixture was centrifuged for 30 min at 14,000 × *g*, 4 °C. Supernatant and pellet fractions contained 14 ± 4 and 83 ± 7% of the total lipid content. Equivalent aliquots were taken from supernatant (corresponding to free protein) and pellet fractions (corresponding to liposome-bound protein), then samples were subjected to reducing SDS-PAGE on 15% Tris-glycine gels. After electrophoresis, proteins from the gel were electroblotted onto 0.2-μm nitrocellulose membranes followed by visualization by Western blotting using appropriate primary antibodies, peroxidase-conjugated secondary antibodies, and enhanced-chemiluminescent (ECL) kit substrates (Pierce). Primary antibodies used for BIM, tBID, and BAX detection were anti-BIM B7929 polyclonal antibody (Sigma), anti-BID MAB860 monoclonal antibody (R&D systems), and anti-BAX N20 polyclonal antibody (Santa Cruz), respectively.

Assays of BAX Oligomerization at MOM-mimetic LUV—For studies of BAX oligomerization, apoptotic proteins were first incubated with MOM-mimetic LUV (100 μM) for 20 min at 37 °C (V_{final} = 100 μl). Then, the amine-reactive disuccinimidyl suberate cross-linker was added at a 0.1 mM concentration followed by incubation of the mixture for 30 min at room temperature and quenching of free cross-linker by the addition of 0.1 volume of 2 M Tris-HCl, pH 7.4. Finally, samples were examined for BAX immunoreactivity as described above.

Monolayer Surface Pressure Measurements—Surface pressure measurements were carried out with a MicroTrough-S system from Kibron (Helsinki, Finland) at 37 °C with constant stirring. Lipid monolayers resembling the composition of MOM contact sites were used ((40 PC/35 PE/10 PI/15 CL (mol/mol)) (MOM-mimetic monolayers). The lipid, dissolved in chloroform and methanol (2:1), was gently spread over the surface of 1 ml of KHE buffer and kept at a constant surface area. The desired initial surface pressure was attained by changing the amount of lipid applied to the air-water interface. After 10 min to allow for solvent evaporation, the protein/peptide was injected through a hole connected to the subphase. The change in surface pressure was recorded as a function of time until a stable signal was obtained. Maximal surface pressures obtained after injecting an excess of protein/peptide in the absence of a lipid monolayer were below initial monolayer pressure values examined.

Far-UV Circular Dichroism (CD) Measurements—Far-UV CD spectra were recorded at 37 °C on a Jasco J-810 spectrapolarimeter (Jasco Spectroscopic Co. Ltd., Hachioji City, Japan) equipped with a Jasco PTC-423S temperature control unit using a 1-mm path length cell. Data were collected every 0.2 nm at 50 nm/min from 250 to 200 nm with a bandwidth of 2 nm, and results were averaged from 20 scans. All samples were allowed to equilibrate for 15 min before measurement. Peptides (5 μM) were mixed with MOM liposomes (500 μM) in 50 mM Na_2HPO_4, 20 mM KCl, pH 7.0. Each spectrum represents the average of three distinct spectral recordings. The contribution of buffer and lipid to the measured ellipticity was subtracted as blank.

Measurements of LUV Size by Quasi-elastic Light Scattering—Vesicle size was determined by quasi-elastic light scattering at a fixed angle of 90° and room temperature using a Malvern Zetasizer 4 instrument (Malvern, UK). A 64-channel correlator was used capable of estimating particle sizes in the range from 5 to 5000 nm. Data were analyzed by the cumulant method using Malvern Application Software. The hydrodynamic radius of the particle was obtained from the first cumulant.

^{31}P NMR Measurements—Samples for ^{31}P NMR were prepared by dispersing 15 μmol of dry MOM-mimetic lipid mixtures in either 0.5 ml of KHE buffer alone or 0.5 ml of KHE buffer containing the protein/peptide of interest at 150 μM concentration. Multilamellar vesicle suspensions were freeze-thawed 3 times in liquid N_2 to disperse the added proteins in the lipid membranes, and the liposomes were spun down in an Eppendorf centrifuge (14,000 rpm, 15 min, 4 °C). Pellets were loaded directly into 5-mm Pyrex NMR tubes. Samples were equilibrated for 20 min at each temperature before data acquisition. High power, proton noise-decoupled ^{31}P NMR spectra were recorded on a Bruker AV-500 spectrometer operating at 202.4 MHz using 5-mm broadband inverse probes with z-gradient equipment. 1024 free induction decays were averaged using a 2-s recycle delay. Spectra were processed and evaluated using TOPSPIN 1.3 (Bruker) and plotted with 80-kHz line broadening.

RESULTS

Truncated BID but Not BIM Potently Triggers the Permeabilizing Function of BAX at Nanomolar Dosing—We previously showed that the BAX-driven MOM permeabilization pathway triggered by tBID can be reconstituted in MOM-mimetic LUV containing entrapped FD70 (32). To gain more insight into the mode of BIM and tBID action, we purified different recombinant forms of these proteins which play prominent roles during many cell death pathways (44, 45) (supplemental Fig. 1). Then we compared the effectiveness of each polypeptide to trigger the permeabilizing function of BAX by performing in parallel quantitative assays for release of cytochrome *c* from isolated rat liver mitochondria and for release of FD70 from MOM-mi-

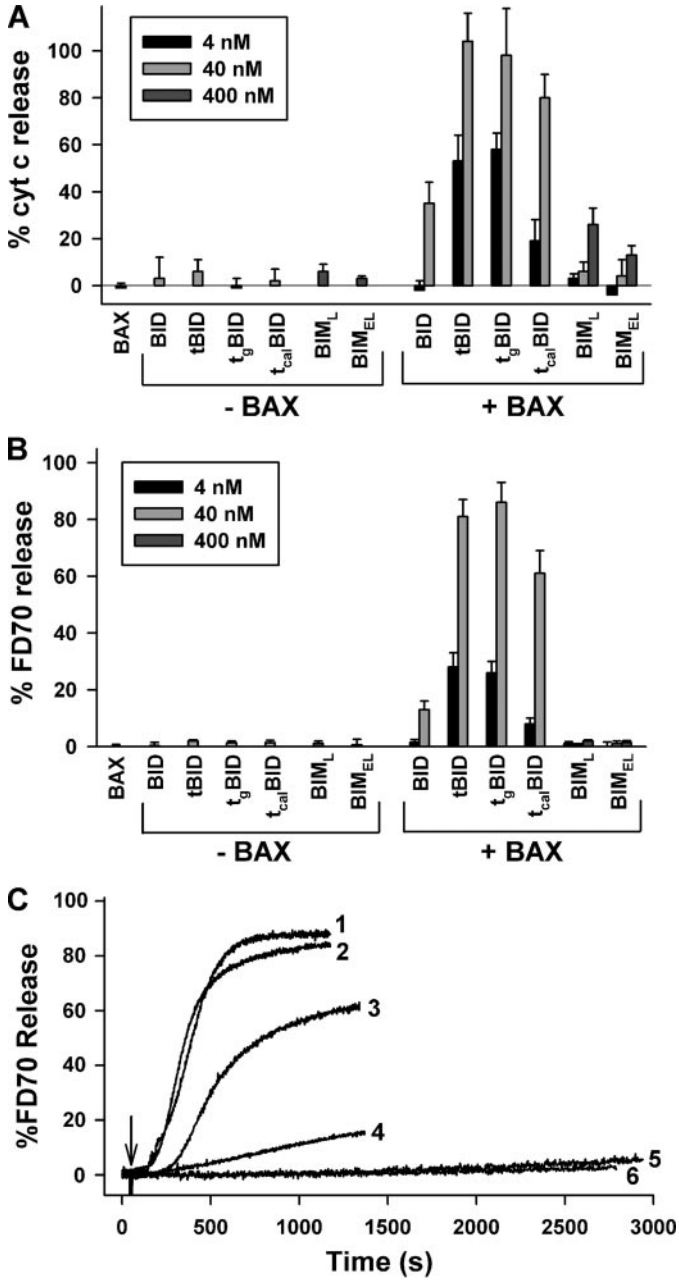

FIGURE 1. **Effect of BAX and of various BID/BIM-derived polypeptides on the release of mitochondrial cytochrome *c* and vesicular FD70.** *A*, rat liver mitochondria were incubated with indicated amounts of recombinant apoptotic proteins for 20 min followed by enzyme-linked immunosorbent assay-based analysis of cytochrome *c* (*Cyt c*) release. Data represent the mean values and S.E. from 2–3 independent experiments. *B*, FD70-loaded MOM-mimetic LUV were treated with the indicated amounts of recombinant apoptotic proteins for 20 min followed by determination of extents of marker release. Data represent the mean values and S.E. from 3–7 independent experiments. *C*, vesicular FD70 release kinetics elicited by indicated apoptotic proteins. *1*, BAX + tBID; *2*, BAX + t_gBID; *3*, BAX + t_{cal}BID; *4*, BAX + BID; *5*, BAX + $BIM_L\Delta C$; *6*, BAX + $BIM_{EL}\Delta C$. *Arrow*, time of protein addition. Concentrations of BAX/truncated BID and $BIM_L\Delta C$/$BIM_{EL}\Delta C$ were 40 and 400 nM, respectively.

metic LUV. At nanomolar dosing, none of the BH3-only proteins by themselves or BAX alone caused substantial release in mitochondrion- or liposome-based systems (Fig. 1, *A* and *B*). However, co-treatment with BAX and truncated BID generated either by caspase 8 (tBID), granzyme B (t_gBID), or calpain (t_{cal}BID) led to a similar dose-responsive release of mitochondrial cytochrome *c* and vesicular FD70 (Fig. 1, *A* and *B*). Mitochondria and liposomes also responded similarly to treatment with uncleaved BID in the presence of BAX, although levels of release were notably lower than those obtained with truncated BID forms. Dextran release triggered by all BID forms was effectively blocked by a specific chemical inhibitor of the BAX pore (Bci-1 (Bax-channel inhibitor 1)) (46), confirming that release of vesicular contents occurred through activation of the permeabilizing function of BAX (supplemental Fig. 2). By contrast to BID-derived polypeptides, even 400 nM concentrations of $BIM_L\Delta C$ and $BIM_{EL}\Delta C$ in combination with BAX failed to produce a comparable mitochondrial cytochrome *c* release. Moreover, unlike BID and truncated BID, submicromolar concentrations of $BIM_L\Delta C$ or $BIM_{EL}\Delta C$ were completely ineffective against MOM-mimetic LUV even after more than doubling the standard incubation time for this assay (Fig. 1, *B* and *C*).

All BID forms examined contain structurally defined membrane-interacting regions (44), whereas $BIM_L\Delta C$ and $BIM_{EL}\Delta C$ lack a C-terminal region with a presumed membrane-targeting function (45). Localization to the membrane may facilitate the functional interaction of BH3-only proteins with BAX, thus providing a potential explanation for the varying levels of dextran release observed with different recombinant proteins. To examine this possibility, BH3-only proteins were incubated with MOM-mimetic liposomes in the presence of BAX then liposome-associated, and liposome-free fractions were separated by centrifugation and immunoblotted for the presence of BID/BIM. As shown in Fig. 2*A*, a general agreement was found between the capacity of different BIM/BID forms to co-fractionate with liposomes and their relative potency to trigger BAX-driven vesicular FD70 release. Studies performed in the absence of BAX confirmed that truncated forms of BID partition more strongly than BIM polypeptides into MOM-mimetic model membranes (supplemental Fig. 3).

Prompted by these observations, we decided to examine whether membrane-targeting confers BIM the ability to trigger BAX-driven membrane permeabilization. To this aim, we employed the polyhistidine-Ni^{2+}-NTA affinity system (47). His_6-tagged BIM polypeptides were incubated with either regular MOM-mimetic liposomes or with MOM-mimetic liposomes containing the Ni^{2+}-chelating lipid analogue DOGS-NTA-Ni. Then liposome-bound and unbound fractions were separated by centrifugation and immunoblotted for BIM. As expected, a large amount of $BIM_L\Delta C$ and $BIM_{EL}\Delta C$ partitioned with DOGS-NTA-Ni-containing liposomes but not with regular liposomes (Fig. 2*B*). The addition of EDTA, which strips Ni^{2+} ion from the NTA moieties of DOGS-NTA-Ni, reduced the amount of liposome-associated $BIM_L\Delta C$ and $BIM_{EL}\Delta C$, demonstrating that His_6-tagged proteins were chemically attached to the Ni^{2+}-chelating lipid analog incorporated into the liposomal membrane. We then examined the ability of increasing concentrations of membrane-bound $BIM_L\Delta C$ and $BIM_{EL}\Delta C$ to trigger the permeabilizing function of BAX in NTA-derivatized MOM-mimetic LUV. In these experiments submicromolar concentrations of BIM proteins were used, which by themselves were not sufficient to bring about vesicular FD70 release. As shown in Fig. 2*C*, liposome-targeted $BIM_L\Delta C$ and $BIM_{EL}\Delta C$ induced considerable vesicular FD70

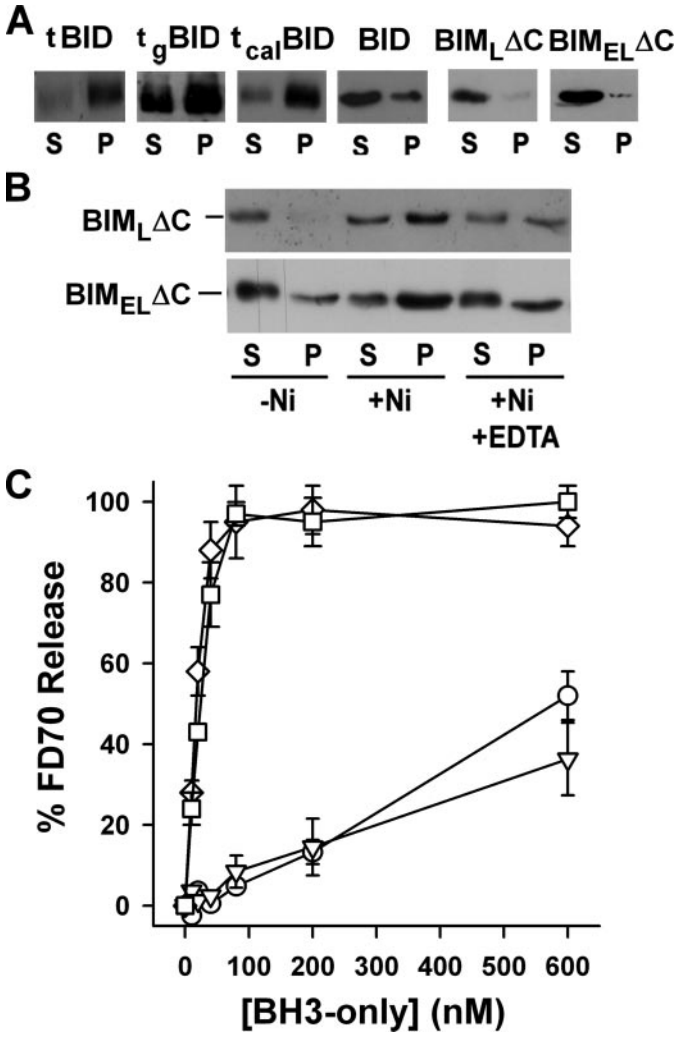

FIGURE 2. **Lipid-interacting properties of different BIM/BID-derived polypeptides.** *A*, freeze/thawed MOM-mimetic liposomes were incubated with indicated proteins (200 nM) together with BAX (200 nM) for 20 min followed by centrifugation of the samples. Equivalent volumes of liposome-free supernatant (*S*) and liposome-containing pellet (*P*) fractions were then subjected to anti-BID or anti-BIM Western blot analysis. *B*, hexahistidine-tagged $BIM_L\Delta C$ and $BIM_{EL}\Delta C$ (200 nM) were co-incubated with BAX and freeze/thawed MOM-mimetic liposomes containing 0 mol% DOGS-NTA-Ni (−*Ni*) or 5 mol% DOGS-NTA-Ni in the absence (+*Ni*) or presence of 10 mM EDTA (+*Ni* +*EDTA*). Samples were centrifuged, and supernatant (*S*) and pellet (*P*) fractions were subjected to anti-BIM Western blot analysis. *C*, effect of $BIM_L\Delta C$ (*circles*), $BIM_{EL}\Delta C$ (*triangles*), tBID (*squares*), and t_gBID (*diamonds*) on the release of FD70 from MOM-mimetic LUV containing 5 mol% DOGS-NTA-Ni in the presence of BAX (40 nM). Data represent the mean values and S.E. from 3–5 independent measurements. When administered alone, all proteins triggered <5% dextran release within this concentration range.

release in the presence of BAX. However, the level of dextran release obtained with the highest concentrations of BIM proteins tested (600 nM) were achieved at about 30-fold lower concentrations of truncated BID proteins (Fig. 2*C*). These data, thus, demonstrate that membrane-targeted BIM polypeptides trigger the permeabilizing function of BAX with much lower potency than truncated forms of BID.

BIM Polypeptides Reverse the Inhibition Exerted by All Anti-apoptotic Proteins on the tBID-triggered Permeabilizing Function of BAX—We previously found that $BIM_{EL}\Delta C$ can contribute to the BAX-driven membrane permeabilization pathway in MOM-mimetic LUV by overcoming BCL-2ΔC inhibition (32). To re-evaluate the validity of this mode of BIM action, we extended our investigations to $BIM_L\Delta C$ as well as to additional antiapoptotic proteins. We first compared the effects of BCL-2ΔC, BCL-WΔC, and A1ΔC, the latter two being BCL-2 homologues for which model membrane studies are lacking. Each antiapoptotic protein inhibited the tBID-triggered permeabilizing function of BAX to a similar degree in isolated mitochondria and MOM-mimetic LUV, further validating this liposomal system as a high fidelity experimental correlate to the mitochondrion (Fig. 3, *A* and *B*). The specificity of the inhibition by BCL-2ΔC, BCL-WΔC, and A1ΔC on BAX-driven liposome permeabilization was confirmed by the inability of antiapoptotic proteins to decrease the release of vesicular contents induced by melittin, a pore-forming peptide, as well as by *S. aureus* α-toxin and tetanolysin, two distinct pore-forming toxins that open proteinaceous channels by inserting a transmembrane β-barrel into the bilayer (supplemental Fig. 4). Interestingly, the relative potency of the three antiapoptotic proteins to inhibit dextran release correlated with their relative affinity for the tBID BH3 motif (7, 8). This finding raised the possibility that antiapoptotic proteins inhibited BAX-induced dextran release at least in part via direct binding interaction between their hydrophobic groove and the tBID BH3 domain. In confirmation of this idea, BCL-2ΔC, BCL-WΔC, and A1ΔC showed a lower capacity to inhibit dextran release when BAX was combined with tBID97A98A, a BH3 domain mutant of tBID with diminished affinity for binding BCL-2-type proteins (Fig. 3*C*) (18, 41). BCL-$X_L\Delta C$ and MCL-1ΔC also inhibited the tBID-triggered permeabilizing function of BAX, confirming previous findings (Table 1) (10), and the 97A98A mutation decreased as well the tBID susceptibility to inhibition by these antiapoptotic proteins (data not shown).

Having demonstrated the general agreement between BCL-2 protein activities on isolated mitochondria and MOM-mimetic LUV, we then used the reconstituted liposome system to examine whether $BIM_L\Delta C$ and $BIM_{EL}\Delta C$ could restore the permeabilizing function of BAX in the presence of inhibitory concentrations of antiapoptotic proteins. In fact, despite their inability to trigger BAX-driven vesicular FD70 release, soluble BIM polypeptides overcome the inhibition of dextran release by all five BCL-2-type proteins (Fig. 4). It is worth noting that whereas equimolar $BIM_L\Delta C$ was sufficient for near-complete reversal of inhibition by BCL-2-type proteins, an excess $BIM_{EL}\Delta C$ was required to overcome fully the inhibitory effect exerted by antiapoptotic proteins (data not shown). The observed difference might be due to conformational constraints present in $BIM_{EL}\Delta C$ that modify the accessibility of its BH3 domain under these experimental conditions (see below).

The Effect Exerted by BIM, but Not tBID, on BAX-permeabilizing Function Can Be Reproduced by a Peptide Representing the BIM BH3 Domain—We next sought to determine the role of the BH3 domain of BIM and BID in triggering the permeabilizing function of BAX. To this aim, we studied the effect of synthetic 21-mer peptides representing the BH3 domains of BIM and BID (see supplemental Table 1 for a list of peptides used in this study). Similar to BIM polypeptides, nanomolar concentrations of the isolated BIM BH3 peptide completely restored BAX-induced vesicular FD70 release in the presence

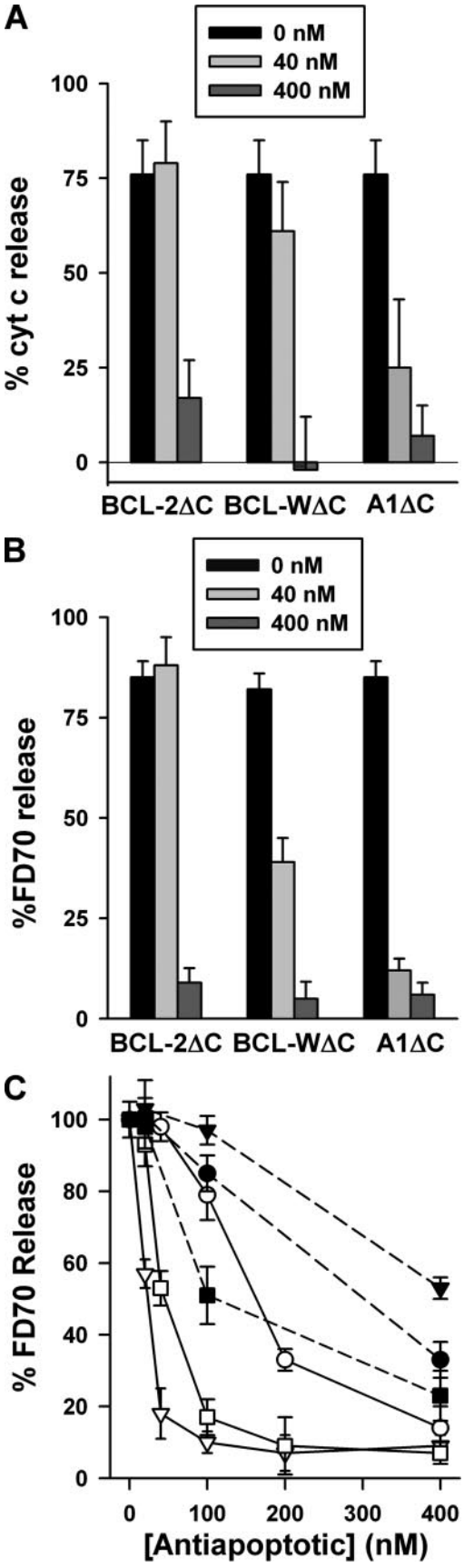

FIGURE 3. **Antiapoptotic proteins inhibit the functional activation of BAX triggered by tBID.** *A*, rat liver mitochondria were treated for 5 min with the indicated amounts of BCL-2ΔC, BCL-WΔC, or A1ΔC before the addition of BAX (40 nM) plus tBID (20 nM), and cytochrome *c* (*Cyt c*) release was measured as explained in Fig. 1*A*. *B*, FD70-loaded MOM-mimetic LUV were treated for 5 min with the indicated amounts of BCL-2ΔC, BCL-WΔC, or A1ΔC before the addition of BAX (40 nM) plus tBID (40 nM), and extents of marker release were determined as explained in Fig. 1*B*. *C*, inhibition by BCL-2ΔC (*circles*), BCL-WΔC (*squares*), and A1ΔC (*triangles*) of the BAX-driven vesicular FD70 release triggered by tBID (*open symbols*, *continuous lines*) or tBID97A98A (*closed symbols*, *discontinuous lines*). Data were normalized to a percentage of the release induced by BAX plus tBID/tBID97A98A, representing mean values and S.E. from 2–4 independent measurements.

of inhibitory concentrations of all five BCL-2-type proteins (Table 1). Furthermore, the isolated BIM BH3 peptide reversed inhibition of dextran release by antiapoptotic proteins with dose dependences lagging slightly behind those exhibited by $BIM_L\Delta C$ (Fig. 5). In contrast, the isolated BID BH3 peptide showed modest capability to overcome inhibition by A1ΔC, BCL-WΔC, and BCL-X_LΔC and was virtually ineffective against BCL-2ΔC and MCL-1ΔC (Fig. 5 and Table 1). These results are in agreement with the measured nanomolar affinity constants of BIM BH3 peptides for the entire set of BCL-2-type proteins as well as with the generally lower affinity and more restricted binding pattern displayed by BID BH3 peptides for prosurvival proteins (8–11). Indeed, BIM/BID BH3 peptides containing mutations known to be critical for binding to prosurvival proteins (9, 10) lost most, if not all, reversing activity (Table 1). Incorporation of regions flanking the BH3 domain of tBID has been proposed to increase the binding affinity of this motif for BCL-2-type proteins (7). However, an extended 29-mer BID BH3 peptide retained a poor capacity to restore dextran release in the presence of BCL-2ΔC and MCL-1ΔC (Table 1). Thus, we concluded that the BH3 domain of BIM, but not of BID, efficiently overcomes the inhibition exerted by all BCL-2-type proteins on the tBID-triggered permeabilizing function of BAX.

Another important outcome of these experiments is our finding that none of the isolated BH3 peptides tested (including 29-mer BID BH3 peptide) had a significant effect on dextran release when combined with BAX alone at submicromolar concentrations (Fig. 5 (*triangles*) and supplemental Fig. 5). In a further examination of whether free BH3 peptides had any ability to induce BAX-mediated membrane permeabilization directly, we combined them with BAX and a suboptimal amount of tBID but did not observe increased dextran release (supplemental Fig. 5). A recent study reported that the BID BH3 peptide acquires the ability to trigger BAX permeabilizing function if attached to the liposome surface due to increased peptide concentration and α-helical conformation at the site of BAX action (*i.e.* the lipid membrane) (17). Because tBID can be naturally myristoylated close to the N-terminal end of its BH3 region (48), we set out to examine whether N-terminal myristoylation confers to BID/BIM BH3 peptides increased potency for triggering the permeabilizing function of BAX. We first used lipid monolayers to evaluate the membrane-interacting properties of myristoylated BIM/BID (MyrBIM/BID) BH3 peptides relative to their unmodified counterparts. As shown in Fig. 6*A*, injection of either MyrBIM BH3 or MyrBID BH3 peptide in the subphase of a MOM-mimetic monolayer spread at 30 millinewtons/m resulted in a similar dose-responsive increase in surface pressure, whereas addition of unmodified

TABLE 1

Effect of BCL-2-type proteins and BIM/BID BH3 peptides on BAX-permeabilizing function triggered by tBID

MOM-mimetic LUV were incubated for 5 min with antiapoptotic proteins (300 nM) in the presence or absence of BH3 peptides (600 nM) followed by the addition of BAX (40 nM) plus tBID (40 nM). Extents of vesicular FD70 release were determined after incubating the mixture for 20 min and were normalized to a value of 1 with BAX + tBID alone. Data represent the mean values and S.E. (parentheses) from 2–8 measurements. mt, mutant; ND, not determined.

Protein	Length (amino acids)	BCL-2ΔC	BCL-X_LΔC	BCL-WΔC	MCL-1ΔC	A1ΔC
None		0.17 (0.02)	0.14 (0.01)	0.11 (0.02)	0.12 (0.01)	0.09 (0.01)
BIMBH3	21	1.01 (0.05)	0.89 (0.31)	0.94 (0.13)	0.98 (0.06)	0.97 (0.15)
BIMBH3mt	21	0.25 (0.02)	0.11 (0.02)	0.19 (0.04)	0.09 (0.03)	0.22 (0.02)
BIDBH3	21	0.22 (0.05)	0.31 (0.04)	0.29 (0.04)	0.11 (0.02)	0.35 (0.06)
BIDBH3mt	21	0.15 (0.03)	ND	0.10 (0.01)	0.09 (0.01)	0.14 (0.02)
BIDBH3	29	0.31 (0.11)	0.83 (0.21)	0.91 (0.16)	0.28 (0.07)	0.79 (0.10)

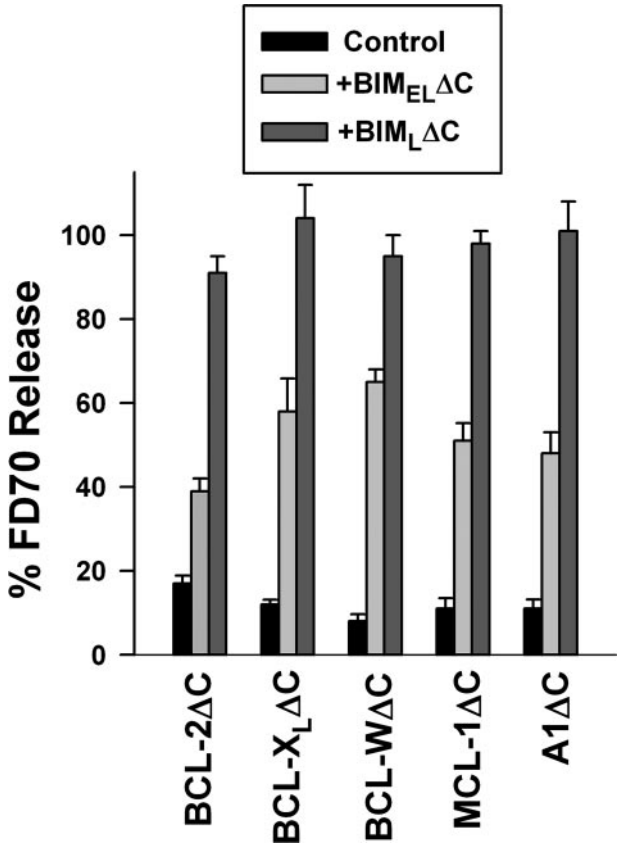

FIGURE 4. **BIM polypeptides reverse the inhibition elicited by antiapoptotic proteins on the BAX permeabilizing function triggered by tBID.** Normalized extents of vesicular FD70 release induced by BAX (40 nM) plus tBID (40 nM) in MOM-mimetic LUV which were pretreated for 5 min with the indicated antiapoptotic proteins (300 nM) in the absence (control) or presence of BIM polypeptides (300 nM). Data represent the mean values and S.E. from 3–4 independent measurements.

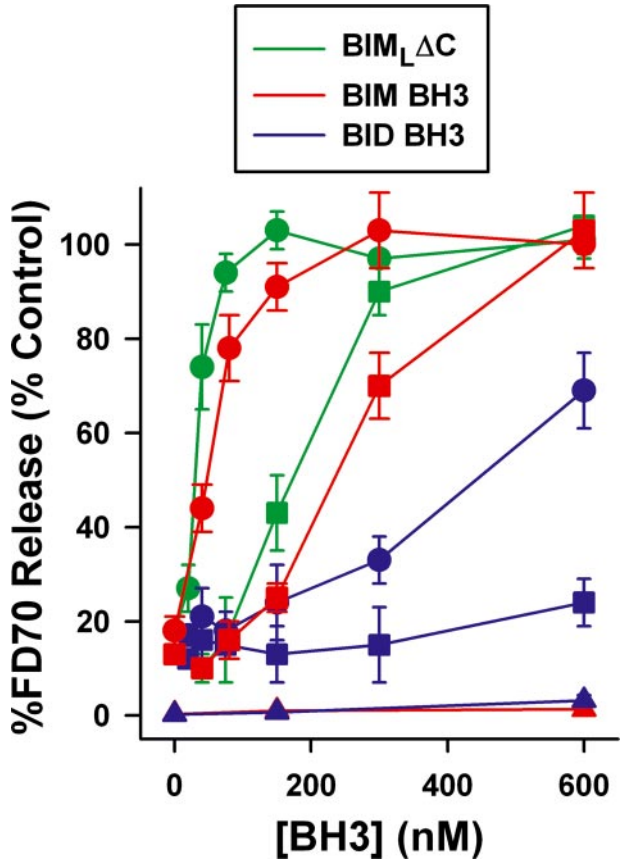

FIGURE 5. **Dose dependence of the effects exerted by BIM$_L$ΔC and BIM/BID BH3 peptides on membrane permeability in the presence of different BCL-2 family members.** Indicated amounts of BIM$_L$ΔC, BIM BH3, or BID BH3 were incubated with FD70-loaded MOM-mimetic LUV for 5 min in the presence of A1ΔC (40 nM) (*circles*), BCL-2ΔC (300 nM) (*squares*), or KHE buffer only (*triangles*). Mixtures were treated with BAX plus tBID (*circles* and *squares*) or BAX alone (*triangles*), and extents of marker release were determined after incubation for 20 min. Data are normalized to a percentage of the release induced by BAX plus tBID (*circles* and *squares*) or BAX alone (*triangles*) and represent the mean values and S.E. from 2–6 independent measurements.

BIM BH3 or BID BH3 peptide had minimal effect. This increase in surface pressure appeared to be primarily due to insertion of the myristoyl moiety and not of the BH3 peptide itself into the monolayer, since the fatty acid alone produced a response similar to that exhibited by myristoylated BH3 peptides. To examine whether N-terminal myristoylation affects peptide secondary structure, myristoylated and unmodified BH3 peptides were incubated with MOM-mimetic LUV, and mixtures were subjected to CD spectroscopy analysis. In the presence of liposomes, the spectrum of myristoylated peptides displayed a pronounced increase in the mean residue molar ellipticity at 222 nm $[\phi]_{222}$, a measure of α-helical content, relative to the spectrum of unmodified peptides (Fig. 6*B*).

Having established that N-terminal myristoylation increases membrane affinity and helicity of BIM/BID BH3 peptides, we then examined the capacity of myristoylated BH3 peptides to trigger directly the BAX permeabilizing function in MOM-mimetic LUV. At submicromolar dosing, both MyrBIM BH3 and MyrBID BH3 peptides induced substantial, yet limited, vesicular FD70 release in the presence of BAX (Fig. 6*C*). Control peptides with mutations in residues predicted to reduce interaction between BIM/BID BH3 motifs and BAX (14, 16) caused minimal dextran release, confirming the specificity of Myr BH3-mediated effects. Remarkably, the dose dependence of myrBIM

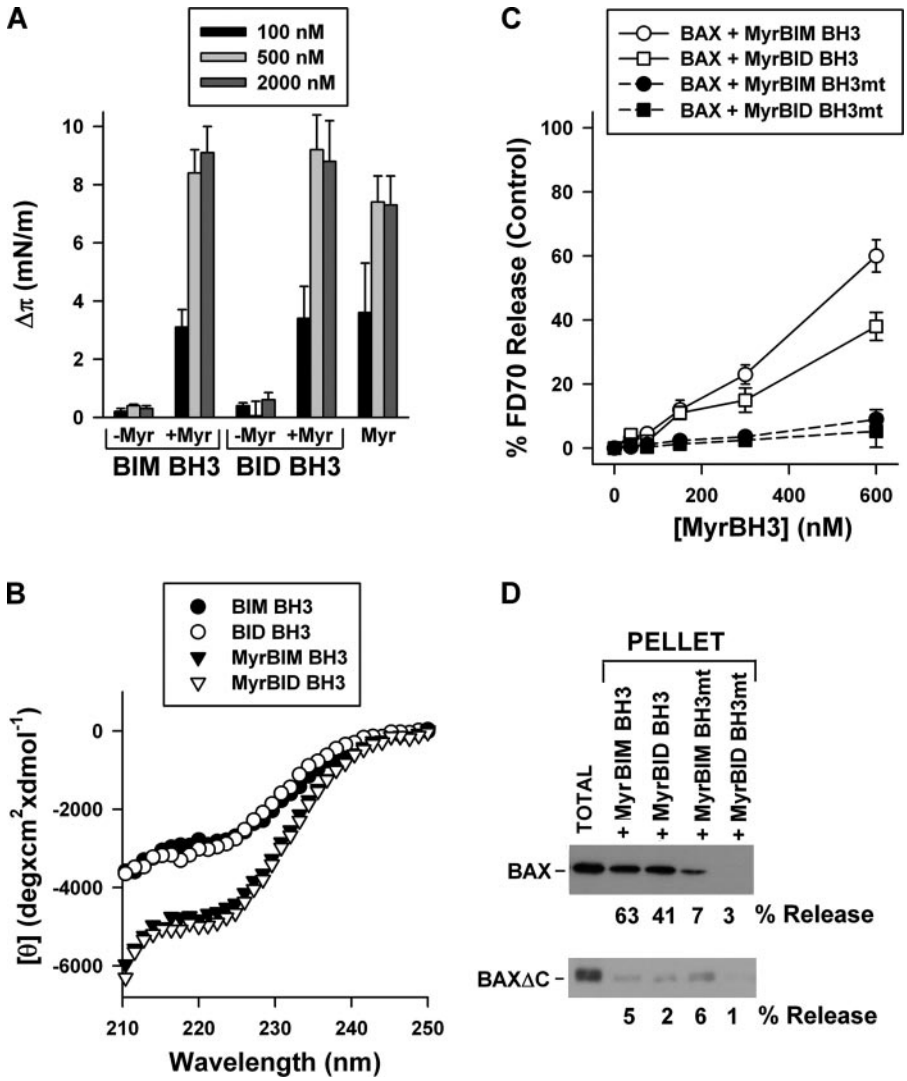

FIGURE 6. **Effect of myristoylated BH3 peptides.** *A*, effects of BID/BIM BH3 peptides with (+*Myr*) or without (−*Myr*) myristic acid attached or myristic acid alone (*Myr*) on the increase of surface pressure of MOM-mimetic monolayers spread at 30 millinewtons/m (±0.3 millinewtons/m). Data represent mean values and S.E. from three independent measurements. No surface pressure change was observed upon injection of either the peptides in the absence of lipid or the peptide solvent (Me_2SO). *B*, CD spectra of indicated peptides incubated with MOM-mimetic LUV. *C*, MOM-mimetic LUV were treated with indicated amounts of MyrBID/BIM BH3 peptides in combination with BAX (40 nM), and extents of marker release were determined after incubation for 20 min. Data represent mean values and S.E. from 3–4 independent measurements. *D*, freeze/thawed MOM-mimetic liposomes were incubated with BAX/BAXΔC (100 nM) combined with indicated peptides (600 nM), liposome-associated fractions were collected by centrifugation, and samples were subjected to anti-BAX immunoblotting. *Total* represents a sample of BAX/BAXΔC (100 nM) without pelleting. % *release* corresponds to mean values of FD70 release obtained from 2–4 measurements (S.E. < 10%).

BH3 on vesicular FD70 release matched well with that of membrane-attached $BIM_L\Delta C$ (compare Fig. 6*C* and Fig. 2*C*). On the other hand, myrBID BH3 triggered vesicular dextran release with much lower potency that truncated BID.

Structural studies revealed the presence in BAX of a C-terminal hydrophobic helix (BAX α9) which folds intramolecularly, occupying the hydrophobic groove presumed to act as a BH3 binding pocket (49). Indeed, it has been shown that emptying the presumptive BH3 binding pocket of BAX by deletion of BAX α9 increases its affinity for BH3-derived peptides (16). Thus, we next asked whether substitution of BAX for C-terminally deleted BAX (BAXΔC) could increase the ability of myristoylated BH3 peptides for triggering the permeabilizing function of BAX. Contrary to this prediction, however, the extent of vesicular FD70 release did not increase but actually decreased when either myrBID BH3 or MyrBIM BH3 were combined with BAXΔC instead of BAX (Fig. 6*D*). Once freed from the rest of the protein, BAX α9 has been shown to function as a transmembrane helix by which the protein can be anchored to the MOM (49). Therefore, one explanation for the above results is that interaction of myristoylated BH3 peptides with BAX, but not BAXΔC, results in BAX α9 exposure, which allows BAX anchoring to the liposome bilayer. Concordant with this logic, myrBIM/BID BH3 peptides induced association of BAX, but not BAXΔC, to MOM-mimetic liposomes (Fig. 6*D*).

Differential Effects of BIM, tBID, and BH3 Peptides on the Permeabilizing Function of Heat-activated BAX—In addition to tBID, other stimuli including a rise in temperature (50) or pH have been proposed to activate the permeabilizing function of BAX. To address this issue, FD70-containing MOM-mimetic LUV were treated with BAX at different temperatures or pH, and the extent of dextran release was quantified. Although incubating MOM-mimetic LUV at 37 °C with 4–200 nM BAX in the pH 7.0–8.5 range had no significant effect on liposome permeability (data not shown), a progressive increase in vesicular contents release was observed when the temperature of the BAX-liposome mixture was increased above 37 °C at neutral pH (Fig. 7*A*). The most evident increase in liposome permeability was observed within the 37–47 °C temperature range, whereas further raising the temperature had less impact, suggesting that 47 °C was nearing the maximal activation of BAX-permeabilizing function. As a negative control, minimal dextran release was observed when liposomes were treated with BAX, which had been pre-heated above its denaturation temperature (~80 °C) (38). We then asked whether prosurvival proteins could inhibit the membrane permeabilization pathway driven by heat-activated BAX. To this end, different antiapoptotic proteins were titrated together with a suboptimal concentration of BAX (40 nM) into FD70-containing MOM-mimetic LUV followed by incubation of the mixture at 47 °C and quantification of dextran

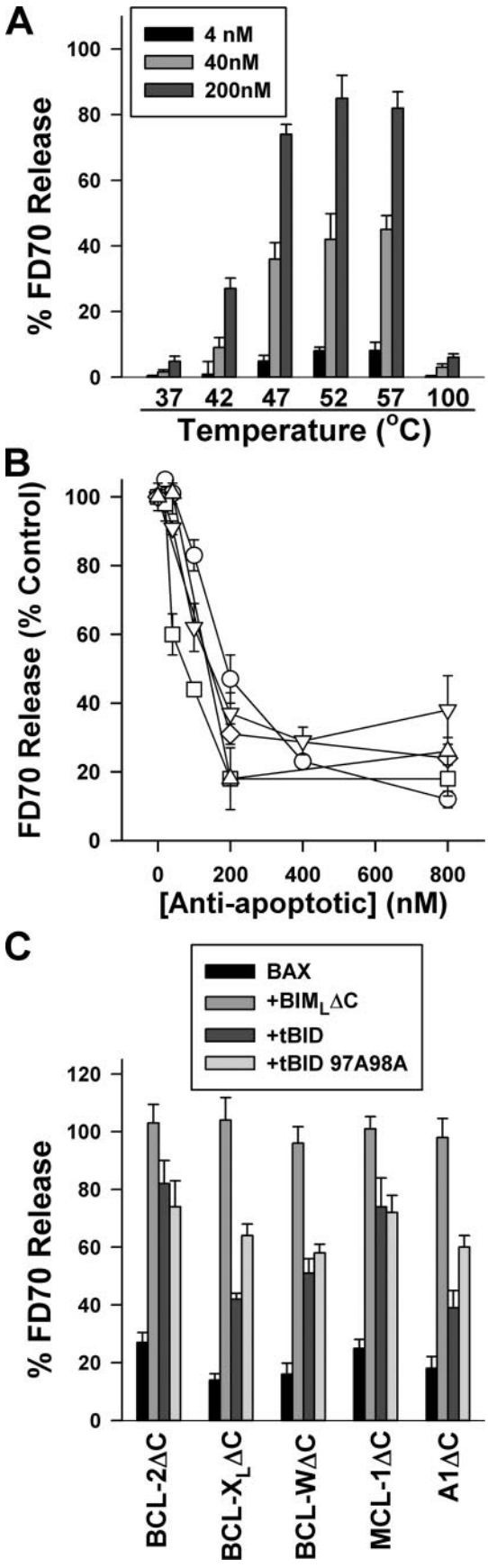

FIGURE 7. **Impact of heat on the regulation of membrane permeability by different BCL-2 family proteins.** *A*, FD70-loaded MOM-mimetic LUV equilibrated for 10 min in the 37–57 °C temperature range were treated with different BAX concentrations, and extents of marker release were determined after a further 20-min incubation. The sample corresponding to 100 °C was prepared by heating BAX at 100 °C for 10 min followed by the addition of the protein to liposomes at 37 °C. Data represent mean values and S.E. from 3–5 independent measurements. *B*, FD70-loaded MOM-mimetic LUV equilibrated at 47 °C were treated for 5 min with increasing amounts of BCL-2ΔC (*circles*), BCL-WΔC (*upward triangles*), A1ΔC (*downward triangles*), BCL-X$_L$ΔC (*squares*), and MCL-1ΔC (*diamonds*). Extents of dextran release were quantified after a further 20-min incubation with a suboptimal concentration of BAX (40 nM). Data are normalized to a percentage of the release induced by BAX alone and represent mean values and S.E. for triplicate measurements. *C*, FD70-loaded LUV equilibrated at 47 °C were treated for 5 min with the indicated proteins (300 nM), and extents of dextran release were quantified after a further 20-min incubation with BAX (40 nM). Data are normalized to a percentage of the release induced by BAX alone and represent mean values and S.E. for 2–5 independent measurements.

TABLE 2

Effect of BCL-2-type proteins and BIM/BID BH3 peptides on BAX-permeabilizing function triggered by heat

MOM-mimetic LUV were incubated for 10 min at 47 °C with antiapoptotic proteins (300 nM) in the presence or absence of BH3 peptides (600 nM) followed by the addition of BAX (40 nM) plus tBID (40 nM). Extents of FD70 release were determined after incubating the mixture for 20 min at 47 °C and were normalized to a value of 1 with BAX + tBID alone. Data represent the mean values and S.E. (parentheses) from 2–4 independent measurements. mt, mutant; ND, not determined.

Protein	BCL-2ΔC	BCL-X$_L$ΔC	BCL-WΔC	MCL-1ΔC	A1ΔC
None	0.26 (0.02)	0.14 (0.01)	0.19 (0.02)	0.22 (0.02)	0.18 (0.02)
BIMBH3	0.97 (0.15)	0.93 (0.11)	1.01 (0.10)	1.03 (0.08)	0.88 (0.23)
BIMBH3mt	0.32 (0.02)	0.21 (0.01)	ND	0.29 (0.04)	0.26 (0.04)
BIDBH3	0.32 (0.04)	0.40 (0.03)	0.34 (0.03)	0.21 (0.02)	0.55 (0.04)
BIDBH3mt	ND	0.21 (0.01)	0.23 (0.01)	ND	0.14 (0.01)

release. As shown in Fig. 7*B*, all antiapoptotic proteins tested reduced the release of vesicular FD70 induced by heat-activated BAX, demonstrating that BCL-2-type proteins can antagonize the membrane permeabilizing activity of BAX without interacting with tBID. Of note, although a controversy exists as to whether MCL-1 can neutralize the BAX proapoptotic function (7, 51, 52), in our liposomal system MCL-1 efficiently inhibited the release of vesicular FD70 induced by heat-activated BAX.

Next, we proceeded to analyze whether BIM and tBID proteins as well as peptides derived from their BH3 domains could reverse the inhibition exerted by antiapoptotic proteins on the permeabilizing function of heat-activated BAX. In the presence of inhibitory concentrations every member of the BCL-2 subgroup, BIM$_L$ΔC fully restored the level of dextran release obtained by heat-activated BAX alone (Fig. 7*C*). This behavior was reproduced by the isolated BIM BH3 peptide (Table 2). In contrast, tBID and the BID BH3 peptide restored dextran release only partially and in the presence of some but not all antiapoptotic proteins (Fig. 7*C* and Table 2). As a measure of specificity, under these conditions neither BH3-only proteins nor BH3 peptides caused considerable vesicular FD70 release by themselves or in combination with antiapoptotic proteins alone (supplemental Fig. 6*A*). Strikingly, the potency of tBID restoring dextran release in the presence of different BCL-2-type proteins did not match the affinity of the tBID BH3 motif for antiapoptotic proteins (Fig. 7*C*) (8). Moreover, despite possessing markedly reduced affinity for antiapoptotic proteins, tBID97A98A behaved similarly to tBID in restoring dextran release (Fig. 7*C*).

One explanation for the effect described above is that tBID enhanced dextran release at 47 °C via direct BH3-BAX interaction. In the next set of experiments, we looked at this possibility

in detail. To this aim, we used tBIDG94A, a BH3 mutant with impaired binding affinity for BAX (7). We first compared the ability of tBID and tBIDG94A in promoting BAX recruitment to MOM-mimetic liposomes at 37 and 47 °C. tBID was clearly more effective than tBIDG94A in promoting the binding of BAX to liposomes at 37 °C, adding support to the idea that tBID BH3-BAX interaction is required to dislodge BAXα9 implicated in membrane anchoring (Fig. 8*A*). Contrarily, BAX itself acquired the capacity to bind to liposomal membranes at 47 °C, and tBID/tBIDG94A did not further augment BAX association with liposomes at this temperature. It is widely believed that in addition to being recruited to the membrane, BAX has to oligomerize to permeabilize the lipid bilayer. Consistently, chemical cross-linking analysis of BAX incubated with MOM-mimetic liposomes at different temperatures revealed that raising the temperature from 37 to 47 °C or above shifted BAX from a monomeric form into higher-order cross-linked complexes with molecular weights corresponding to dimers, trimers, and very large aggregates of the protein (supplemental Fig. 6*B*). However, treatment of liposomes with tBID or tBIDG94A did not cause further changes in the oligomerization pattern of BAX at 47 °C (Fig. 8*C*). Finally, we assessed whether tBID and/or tBIDG94A had any effect in the permeabilizing activity of BAX at 47 °C. Remarkably, both tBID and tBIDG94A caused an increase in the extent of vesicular FD70 release in the presence of BAX at 47 °C (Fig. 8*D*), whereas this effect was not observed with the BID BH3 peptide or with $BIM_L\Delta C$ (supplemental Fig. 6*C*). The enhancement of dextran release induced by tBID/tBIDG94A occurred through the BAX-driven membrane permeabilization pathway rather than via an alternative leakage mechanism since it was blocked by Bci-1 (supplemental Fig. 6*C*). These findings led us to two conclusions. First, in the absence of antiapoptotic proteins, tBID can potentiate the permeabilizing function of heat-activated BAX utilizing a BH3-independent mechanism. Second, tBID does not seem to exert this effect by promoting BAX translocation to or oligomerization at the liposomal membrane.

tBID Disrupts the Lipid Bilayer Structure of MOM-mimetic Liposomes through a BH3-independent and CL-specific Mechanism—In addition to the BH3 domain, a second functional motif has been identified in tBID providing high affinity to the protein for binding CL (25). Complexation of tBID with CL has been shown to modify the function of different mitochondrial proteins via changes in membrane organization (23, 26–29, 53). Thus, we hypothesized that this mode of tBID action might explain how tBID potentiates the permeabilizing function of heat-activated BAX in our liposomal system. As a test for this hypothesis, we compared the response of FD70-loaded LUV containing different proportions of CL to tBID after treating the liposomes with heat-activated BAX. tBID potentiated the release of vesicular FD70 induced by heat-activated BAX through a mechanism dependent on the level of CL present in the liposomal membrane (Table 3). Moreover, tBID was less efficient, amplifying vesicular FD70 release when PI was used instead of CL while maintaining the negative charge of the liposome, indicating that this effect is not simply due to alteration of membrane electrostatic energy.

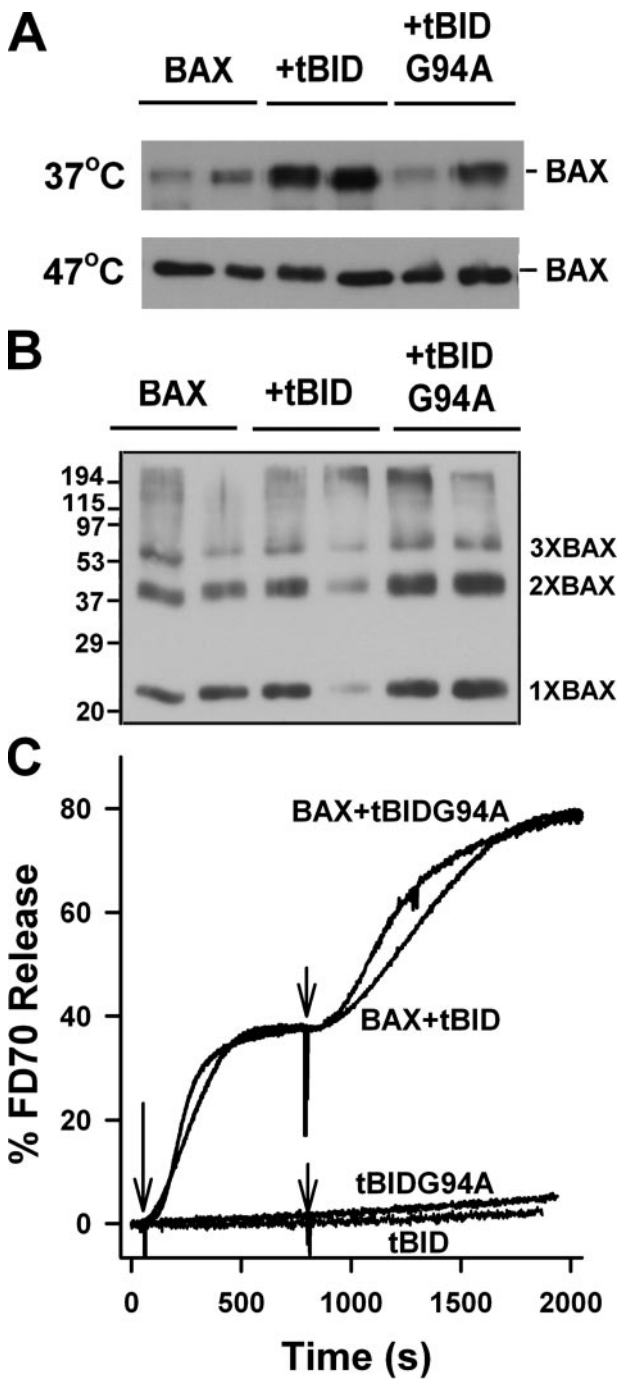

FIGURE 8. **Effect of tBID and tBIDG94A on different stages of the BAX-driven membrane permeabilization pathway.** *A*, freeze-thawed MOM-mimetic liposomes were incubated for 20 min with BAX (100 nM) and tBID/tBIDG94A (500 nM) at indicated temperatures, liposome-containing fractions were collected by centrifugation, and samples were subjected to anti-BAX western-blot analysis. The immunoblot shows samples analyzed in duplicate. *B*, oligomerization of BAX at MOM-mimetic LUV. BAX (100 nM) was incubated with liposomes at 47 °C in the presence or absence of tBID/tBIDG94A (500 nM) followed by treatment with disuccinimidyl suberate and anti-BAX Western blot analysis. The immunoblot shows samples analyzed in duplicate. *C*, FD70-loaded MOM-mimetic LUV were treated at 47 °C as follows: *BAX + tBID*, first 40 nM BAX (*large arrow*) and then 200 nM tBID (*short arrow*); *tBID*, first BAX buffer (*large arrow*) and then 200 nM tBID (*short arrow*); *BAX + tBIDG94A*, first 40 nM BAX (*large arrow*) and then 200 nM tBIDG94A (*short arrow*); *tBIDG94A*, first BAX buffer (*large arrow*) and then 200 nM tBIDG94A (*short arrow*). Experiments were repeated several times independently, yielding virtually identical results.

TABLE 3

Effect of anionic lipids on BAX permeabilizing function triggered by tBID and on tBID-induced changes in lipid bilayer structure and vesicle size distribution

Lipid composition	FD70 release[a]	Isotropic peak[b]	Size[c]
			μM
0% CL	1.08	−	1.41 ± 0.32
3.75% CL	1.13 ± 0.12	−	1.30 ± 0.51
7.5% CL	1.47 ± 0.18[d]	+	1.12 ± 0.24
15% CL	1.92 ± 0.17[d]	++	1.57 ± 0.44
30% PI	1.23 ± 0.16	+	1.23 ± 0.53

[a] Extents of FD70 release induced by BAX (40 nM) + tBID (200 nM) at 47 °C in PC/PE/PI (55/35/10) LUV in which the indicated amounts of anionic lipids were substituted for PC. Data were normalized to a value of 1 with BAX (40 nM) alone. Data represent the mean values ± S.D.

[b] Relative amount of isotropic/bilayer ^{31}P NMR signal in different lipid mixtures containing tBID after incubation for 1 h at 47 °C.

[c] Hydrodynamic radius (mean ± S.E.) of vesicles used for ^{31}P NMR studies.

[d] Indicates p values ≤0.01 when a 2-tailed t test was performed comparing the results obtained with/without tBID.

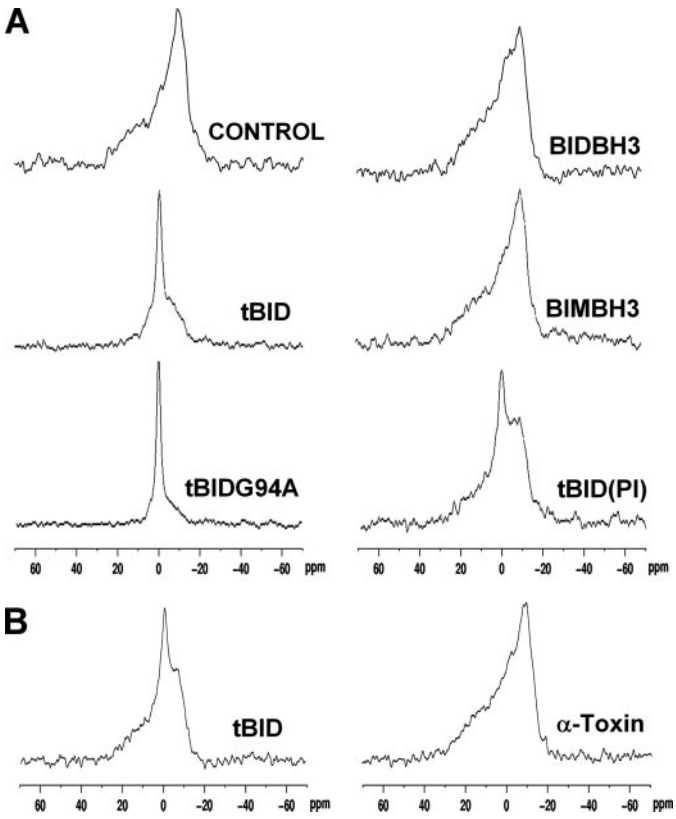

FIGURE 9. **tBID perturbs the membrane bilayer structure in a BH3-independent and CL-specific manner.** *A*, ^{31}P NMR spectra of MOM-mimetic liposomes and of liposomes composed of 25PC/35PE/40PI (*PI*) after incubation with the indicated proteins/peptides or buffer alone (*Control*) for 1 h at 37 °C. In all cases protein/peptide to lipid mol/mol ratio was 1/200. *B*, ^{31}P NMR spectra of MOM-mimetic liposomes and of liposomes composed of 50DOPC/50CHOL after incubation with tBID or with α-toxin, respectively, for 1 h at 37 °C. The protein/lipid mol/mol ratio was 1/800.

Studies of the macroscopic organization of phospholipids interacting with tBID are of relatively a recent date and have been limited until now to phospholipid mixtures containing unphysiologically high concentrations of CL and calcium (37). To examine whether tBID affects the supramolecular organization of phospholipids in our reconstituted liposome system, we conducted ^{31}P NMR assays. As shown in Fig. 9*A*, the ^{31}P NMR of pure MOM-mimetic liposomes shows the high field peak and low field shoulder typical of a bilayer arrangement of membrane lipids. Upon the addition of tBID, however, the shape of the spectrum changed dramatically; the bilayer-type signal markedly decreased, although a prominent peak appeared around the chemical shift position of phospholipids experiencing isotropic motion (Fig. 9*A*). A similar response was obtained with tBIDG94A, whereas neither BID BH3 nor BIM BH3 peptides induced noticeable changes in the bilayer spectrum. It should be noted, however, that the lack of effect of BH3 peptides may simply reflect their inability to partition into the liposomes (see Fig. 6*A*). The isotropic signal was observed at tBID/lipid mol/mol ratios as low as 1/800, whereas incorporation of equivalent amounts of α-toxin into the liposomes did not alter the bilayer spectrum (Fig. 9*B*).

Another point of interest is the lipid specificity of this phenomenon. Indeed, the contribution of the isotropic component to the spectrum gradually increased with the proportion of CL in a manner that correlated qualitatively with CL impact on tBID-mediated amplification of dextran release (Table 3). Further agreement between the appearance of the isotropic resonance and tBID-mediated dextran release was found in that substitution of CL for PI in the MOM-mimetic lipid mixture led to a predominance of the lamellar ^{31}P NMR spectra over the isotropic signal (Fig. 9*A*).

Small vesicles, micelles, small bilayer discs, and certain nonlamellar lipid structures (rhombic, cubic, or inverted micellar) have all been shown to give rise to isotropic ^{31}P NMR signals (54). Although ^{31}P NMR is not capable of discriminating which of these lipid structures is at the origin of the isotropic motion of phospholipids detected in tBID-treated mixtures, the first three possibilities seem less likely on account of the fact that samples were subjected to a short centrifugation step to collect the phospholipid before ^{31}P NMR analysis. The interpretation that isolated small lipid structures are not the cause of the isotropic signal of the ^{31}P NMR spectrum is reinforced by the observation that vesicles with different lipid compositions treated with tBID showed similar size distributions, as assessed by quasi-elastic light scattering (Table 3). Nevertheless, it remains possible that the isotropic signal observed in tBID-treated samples arises from a population of small lipid particles mixed in with the liposome population.

DISCUSSION

In this study we used a reconstituted liposomal system to learn more about the molecular mechanisms by which BIM and tBID trigger BAX-driven MOMP. Using this reduced and biochemically accessible model system, we systematically explored how the BAX-driven membrane permeabilization pathway is influenced by the interactions of BIM/BID-derived polypeptides and BH3 peptides with multidomain BCL-2 family members and with membrane lipids.

According to one currently prominent view, BIM and tBID potently promote apoptosis by binding to and neutralizing all BCL-2 type proteins via their BH3 domains, thereby indirectly triggering BAX function (7). This so-called displacement model originated from structural and biochemical studies revealing that BH3 peptides from different BH3-only proteins behave like

ligands in binding to a hydrophobic groove on the surface of antiapoptotic proteins (8). We obtained three main lines of evidence in our studies with MOM-mimetic liposomes supporting the validity of this model to explain how BIM assists BAX in membrane permeabilization. First, we found that nanomolar dosing of $BIM_L\Delta C$ effectively overcomes the inhibition exerted by five different BCL-2-type protein on the vesicular FD70 release induced by BAX. Additionally, a peptide representing the BIM BH3 domain recapitulated the function of the $BIM_L\Delta C$ protein restoring BAX permeabilizing function in the presence of each one and every BCL-2-type protein. Last, we confirmed that mutations in residues known to be crucial for BIM BH3 binding to hydrophobic grooves on prosurvival proteins abrogated the reversing activity of the BIM BH3 peptide in this reconstituted liposomal system. These results are in line with measured high affinity interactions between $BIM_L\Delta C$ and BCL-2-type proteins (8) as well as with the known capacity of peptides derived from the BIM BH3 motif to mimic parent proteins in binding the entire group of prosurvival proteins (7, 8, 11).

Alternatively, the so-called direct model posits that BIM induces strong apoptosis due to its capacity to directly interact with BAX via its BH3 domain, leading to activation of the BAX-driven membrane permeabilizing pathway (9–11, 14, 16–18). Using a reconstituted liposomal system similar to ours, Kuwana *et al.* (10) previously provided support for this proposal by showing that a free BIM BH3 peptide activated the permeabilizing function of BAX at micromolar concentrations in the absence of antiapoptotic proteins. We now report that not only the BIM BH3 motif but also BIM polypeptides can trigger the permeabilizing function of BAX without involvement of prosurvival relatives in MOM-mimetic LUV. Additionally, our data revealed that BIM BH3 displaces BAX α9 from the rest of the protein, thereby allowing recruitment of BAX to the liposomal membrane. However, in our hands, BIM (poly)peptides had to be artificially targeted to the surface of the liposome to exert these effect, and even under such conditions they only achieved partial activation of BAX permeabilizing function at nanomolar concentrations. Thus, based on these data, it appears unlikely that the BIM BH3-BAX interaction is the principal mechanism by which BIM triggers the BAX-permeabilizing function with high potency during apoptosis.

In contrast to BIM, neither tBID nor BID BH3 peptides could reverse the inhibition exerted by all five different BCL-2-type proteins on BAX-induced vesicular FD70 release at submicromolar concentrations. Although these results contradict the mode of tBID action proposed in the displacement model (7), they are in agreement with reports showing that BID BH3 displays a more restricted binding pattern for BCL-2 type proteins than BIM BH3 (8, 10). On the other hand, at low to mid-nanomolar concentrations, tBID potently triggered the BAX-permeabilizing function in MOM-mimetic LUV without participation of antiapoptotic proteins. As in the case of BIM, our data are consistent with the notion that direct binding interaction between the tBID BH3 motif and BAX displaces BAX α9, thus allowing translocation of the protein to the liposomal membrane. However, the finding that a BID BH3 peptide with optimized membrane targeting capability and bioactive conformation did not reproduce the high potency of the parent tBID polypeptide strongly suggests that this is not the only mechanism by which tBID assists BAX in membrane permeabilization. In apparent contradiction with our results, Oh *et al.* (17) reported that tethering a BID BH3 peptide to the liposomal surface via Ni^{2+}-His_6 interaction recapitulated almost entirely the high potency activation of BAX elicited by tBID. Nevertheless, two important differences between these studies should be pointed out. First, Oh *et al.* (17) incubated BH3 peptides with liposomes for a considerably longer time (1–2 h) than we did (10–20 min). Second, the dextrans used as markers for membrane permeabilization in that study (FD10) were of smaller size than in this one (FD70). Of note, we selected the incubation time for liposome release assays taking into account the period required for complete release of mitochondrial cytochrome *c* by the tBID-BAX combination (Fig. 1*A*), whereas our choice of FD70 was based on the fact that BAX-driven MOMP is characterized by the simultaneous release of cytochrome *c* together with other larger mitochondrial proteins (55).

tBID has been proposed to alter the function of a variety of mitochondrial proteins without physical complexation via interactions with CL (23, 24, 27–29, 53). Along this line of reasoning, we previously reported that the CL binding domain of tBID (lacking the BH3 domain) can enhance the permeabilizing activity of octylglucoside-activated BAX in MOM-mimetic LUV (32). The results of the present work show that (i) tBID can amplify the permeabilizing function of heat-activated BAX independently of tBID BH3-BAX interaction, (ii) tBID, but not its BH3 domain, disrupts the lipid bilayer structure, and (iii) the BH3-independent effects exerted by tBID on membrane permeability and on bilayer structure are qualitatively correlated with respect to their requirement for CL. Taken together, the above data lead us to hypothesize that, in addition to unmasking BAX α9 via insertion of BID BH3 into the BAX hydrophobic groove, tBID also assists BAX in permeabilizing membranes by producing a destabilizing distortion of the bilayer structure via interaction with CL.

There may be several explanations for how the CL-dependent bilayer-disrupting activity of tBID contributes to the BAX-driven membrane permeabilization pathway. Because BAX is thought to permeabilize membranes by forming pores containing lipids in a non-bilayer configuration (30–33, 40, 56), one possibility is that tBID bilayer-perturbing activity facilitates formation/expansion of the proteolipidic pore itself. Within this framework, we have previously speculated that tBID may impose the positive curvature stress in membrane monolayers required for bending them into a large proteolipidic pore (32, 57). However, the well known ability of CL monolayers to adopt negatively curved morphologies upon charge neutralization by polycationic peptides/proteins is compatible with tBID exerting negative, not positive monolayer curvature stress in CL-enriched membranes (58). Nevertheless, tBID may disrupt the membrane bilayer structure by changing composition-dependent properties of the bilayer other than monolayer curvature in such a manner as to facilitate BAX-driven lipidic pore formation/expansion. tBID has been shown to adopt a fold in the membrane similar to that observed in many amphipathic antimicrobial peptides (59). After current models on the mechanism of action of antimicrobial peptides, intercalation of

amphipathic tBID helices between CL head groups on the outer monolayer of the membrane may produce membrane lateral tension known to favor enlargement of lipid-containing pores (60–62). It is also conceivable that the tBID-CL interaction promotes formation of CL-enriched lipid domains (23, 28) and that this phenomenon is somehow linked to opening/expansion of proteolipidic BAX pore.

Alternatively, changes in bilayer architecture promoted by tBID-CL interaction may act as a mediator in the functional activation of BAX by promoting a conformational change in BAX at the level of the membrane that increases its permeabilizing activity. For instance, a localized destabilization of the bilayer structure induced by the interaction of tBID with CL may lower the energetic cost for inserting amphipathic segments of BAX into the lipid matrix of the membrane. Of note, a similar proposal has been made recently to explain how specific components of the complement system cooperate at the plasma membrane level to breach this permeability barrier (63).

In summary, based on the results of this paper, we wish to propose that BIM and tBID follow different strategies to achieve optimal triggering of BAX-driven MOMP and apoptosis. On the one hand, the primary cause of the highly lethal activity of BIM would be the versatility of its BH3 domain to bind to and neutralize all antiapoptotic BCL-2-type proteins. On the other hand, the potent proapoptotic effect of tBID would predominantly arise from its strong capacity to assist BAX in membrane permeabilization via both BH3- and CL-mediated interactions. The reconstituted liposome system described here may provide a powerful tool with which to gain additional mechanistic insights into the functional interplay between the various subclasses of BCL-2 family proteins.

Acknowledgments—We thank David Huang (The Walter and Eliza Hall Institute of Medical Research, Parkville, Australia) and Hong-Gang Wang (H. Lee Moffitt Cancer Center, Tampa, FL) for providing plasmids for expression of recombinant proteins, Dr. Felix M. Goñi and Dr. Jose L. Nieva for critical reading of the manuscript, and M. I. Collado from the NMR service of the Universidad del Pais Vasco/Euskal Herriko Unibertsitatea for technical assistance with ^{31}P NMR experiments.

REFERENCES

1. Green, D. R., and Kroemer, G. (2004) *Science* **305,** 626–629
2. Youle, R. J., and Strasser, A. (2008) *Nat. Rev. Mol. Cell Biol.* **9,** 47–59
3. Leber, B., Lin, J., and Andrews, D. (2007) *Apoptosis* **12,** 897–911
4. Mizuta, T., Shimizu, S., Matsuoka, Y., Nakagawa, T., and Tsujimoto Y. (2007) *J. Biol. Chem.* **282,** 16623–16630
5. Galonek, H. L., and Hardwick, J. M. (2006) *Nat. Cell Biol.* **8,** 1317–1319
6. Youle, R. J. (2007) *Science* **315,** 776–777
7. Willis, S. N., Fletcher, J. I., Kaufmann, T., van Delft, M. F., Chen, L., Czabotar, P. E., Ierino, H., Lee, E. F., Fairlie, W. D., Bouillet, P., Strasser, A., Kluck, R. M., Adams, J. M., and Huang, D. C. (2007) *Science* **315,** 856–859
8. Chen, L., Willis, S. N., Wei, A., Smith, B. J., Fletcher, J. I., Hinds, M. G., Colman, P. M., Day, C. L., Adams, J. M., and Huang, D. C. S. (2005) *Mol. Cell* **17,** 393–403
9. Letai, A., Bassik, M. C., Walensky, L. D., Sorcinelli, M. D., Weiler, S., and Korsmeyer, S. J. (2002) *Cancer Cell* **2,** 183–192
10. Kuwana, T., Bouchier-Hayes, L., Chipuk, J. E., Bonzon, C., Sullivan, B. A., Green, D. R., and Newmeyer, D. D. (2005) *Mol. Cell* **17,** 525–535
11. Certo, M., Del Gaizo Moore, V., Nishino, M., Wei, G., Korsmeyer, S. J., Armstrong, S. A., and Letai, A. (2006) *Cancer Cell* **9,** 351–365
12. Petros, A. M., Olejniczak, E. T., and Fesik, S. W. (2004) *Biochim. Biophys. Acta* **1644,** 83–94
13. Day, C. L., Chen, L., Richardson, S. J., Harrison, P. J., Huang, D. C. S., and Hinds, M. G. (2005) *J. Biol. Chem.* **280,** 4738–4744
14. Liu, X., Dai, S., Zhu, Y., Marrack, P., and Kappler, J. W. (2003) *Immunity* **19,** 341–352
15. Denisov, A. Y., Chen, G., Sprules, T., Moldoveanu, T., Beauparlant, P., and Gehring, K. (2006) *Biochemistry* **45,** 2250–2256
16. Walensky, L. D., Pitter, K., Morash, J., Oh, K. J., Barbuto, S., Fisher, J., Smith, E., Verdine, G. L., and Korsmeyer, S. J. (2006) *Mol. Cell* **24,** 199–210
17. Oh, K. J., Barbuto, S., Pitter, K., Morash, J., Walensky, L. D., and Korsmeyer, S. J. (2006) *J. Biol. Chem.* **281,** 36999–37008
18. Kim, H., Rafiuddin-Shah, M., Tu, H. C., Jeffers, J. R., Zambetti, G. P., Hsieh, J. J. D., and Cheng, E. H.-Y. (2006) *Nat. Cell Biol.* **8,** 1348–1358
19. Terradillos, O., Montessuit, S., Huang, D. C., and Martinou, J. C. (2002) *FEBS Lett.* **522,** 29–34
20. Hinds, M. G., Smits, C., Fredericks-Short, R., Risk, J. M., Bailey, M., Huang, D. C., and Day, C. L. (2006) *Cell Death Differ.* **14,** 128–136
21. Weber, A., Paschen, S. A., Heger, K., Wilfling, F., Frankenberg, T., Bauerschmitt, H., Seiffert, B. M., Kirschnek, S., Wagner, H., and Hacker, G. (2007) *J. Cell Biol.* **177,** 625–636
22. Guscetti, F., Nandita, N., and Denko, N. (2005) *FASEB J.* **19,** 464–466
23. Gonzalvez, F., Pariselli, F., Dupaigne, P., Budihardjo, I., Lutter, M., Antonsson, B., Diolez, P., Manon, S., Martinou, J. C., Goubern, M., Wang, X., Bernard, S., and Petit, P. X. (2005) *Cell Death Differ.* **12,** 614–626
24. Gonzalvez, F., Bessoule, J.-J., Rocchiccioli, F., Manon, S., and Petit, P. X. (2005) *Cell Death Differ.* **12,** 659–667
25. Lutter, M., Fang, M., Luo, X., Nishijima, M., Xie, X., and Wang, X. (2000) *Nat. Cell Biol.* **2,** 754–761
26. Kim, T. H., Zhao, Y., Ding, W. X., Shin, J. N., He, X., Seo, Y. W., Chen, J., Rabinowich, H., Amoscato, A. A., and Yin, X. M. (2004) *Mol. Biol. Cell* **15,** 3061–3072
27. Liu, J., Weiss, A., Durrant, D., Chi, N. W., and Lee, R. M. (2004) *Apoptosis* **9,** 533–541
28. Giordano, A., Calvani, M., Petillo, O., Grippo, P., Tuccillo, F., Melone, M. A., Bonelli, P., Calarco, A., and Peluso, G. (2005) *Cell Death Differ.* **12,** 603–613
29. Tyurin, V. A., Tyurina, Y. Y., Osipov, A. N., Belikova, N. A., Basova, L. V., Kapralov, A. A., Bayir, H., and Kagan, V. E. (2007) *Cell Death Differ.* **14,** 872–875
30. Basañez, G., Zhang, J., Chau, B. N., Maksaev, G. I., Frolov, V. A., Brandt, T. A., Burch, J., Hardwick, J. M., and Zimmerberg, J. (2001) *J. Biol. Chem.* **276,** 31083–31091
31. Basañez, G., Sharpe, J. C., Galanis, J., Brandt, T. B., Hardwick, J. M., and Zimmerberg, J. (2002) *J. Biol. Chem.* **277,** 49360–49365
32. Terrones, O., Antonsson, B., Yamaguchi, H., Wang, H.-G., Liu, Y., Lee, R. M., Herrmann, A., and Basañez, G. (2004) *J. Biol. Chem.* **279,** 30081–30091
33. Polster, B. M., Basañez, G., Young, M., Suzuki, M., and Fiskum, G. (2003) *J. Neurosci.* **23,** 2735–2743
34. Thuduppathy, G. R., Terrones, O., Craig, J. W., Basañez, G., and Hill, R. B. (2006) *Biochemistry* **45,** 14533–14542
35. Antonsson, B., Montessuit, S., Lauper, S., Eskes, R., and Martinou, J.-C. (2000) *Biochem. J.* **345,** 271–278
36. Roucou, X., Montessuit, S., Antonsson, B., and Martinou, J.-C. (2002) *Biochem. J.* **368,** 915–921
37. Epand, R. F., Martinou, J. C., Fornallaz-Mulhauser, M., Hughes, D. W., and Epand, R. M. (2002) *J. Biol. Chem.* **277,** 32632–32639
38. Yethon, J. A., Epand, R. F., Leber, B., Epand, R. M., and Andrews, D. W. (2003) *J. Biol. Chem.* **278,** 48935–48941
39. Tan, C., Dlugosz, P. J., Peng, J., Zhang, Z., Lapolla, S. M., Plafker, S. M., Andrews, D. W., and Lin, J. (2006) *J. Biol. Chem.* **281,** 14764–14775
40. Garcia-Saez, A. J., Coraiola, M., Dalla Serra, M., Mingarro, I., Menestrina, G., and Salgado, J. (2005) *Biophys. J.* **88,** 3976–3990
41. Desagher, S., Osen-Sand, A., Nichols, A. Eskes, R., Montessuit, S. Lauper, S., Maundrell, K., Antonsson, B., and Martinou, J.-C. (1999) *J. Cell Biol.*

144, 891–901
42. Yamaguchi, H., and Wang, H. G. (2002) *J. Biol. Chem.* **277,** 41604–41612
43. Day, C. L., Dupont, C., Lackmann, M., Vaux, D. L., and Hinds, M. G. (1999) *Cell Death Differ.* **6,** 1125–1132
44. O'Connor, L., Strasser, A., O'Reilly, L. A., Hausmann, G., Adams, J. M., Cory, S., and Huang, D. C. (1998) *EMBO J.* **17,** 384–395
45. Yin, X. M. (2006) *Gene* (*Amst.*) **15,** 369–377
46. Hetz, C., Vitte, P.-A., Bombrun, A., Rostovtseva, T. K., Montessuit, S., Hiver, A., Schwarz, M. K., Church, D. J., Korsmeyer, S. J., Martinou, J. C., and Antonsson, B. (2006) *J. Biol. Chem.* **280,** 42960–42970
47. Schmitt, L., Dietrich, L., and Tampe, R. (1994) *Am. Chem. Soc.* **166,** 8485–8491
48. Zha, J., Weiler, S., Oh, K. J., Wei, M. C., and Korsmeyer, S. J. (2000) *Science* **290,** 1761–1765
49. Suzuki, M., Youle, R. J., and Tjandra, N. (2000) *Cell* **103,** 645–654
50. Pagliari, L. J., Kuwana, T., Bonzon, C., Newmeyer, D. D., Tu, S., Beere, H. M., and Green, D. R. (2005) *Proc. Natl. Acad. Sci. U. S. A.* **102,** 17975–17980
51. Germain, M., Milburn, J., and Duronio, V. (2008) *J. Biol. Chem.* **283,** 6384–6392
52. Zhai, D., Jin, C., Huang, Z., Satterthwait, A. C., and Reed, J. C. (Jan. 4, 2008) *J. Biol. Chem.* 10.1074/jbc.M708426200
53. Rostovtseva, T. K., Antonsson, B., Suzuki, M., Youle, R. J., Colombini, M., and Bezrukov, S. M. (2004) *J. Biol. Chem.* **279,** 13575–13583
54. Cullis, P. R., Hope, M. J., de Kruijff, B., Verkleij, A. J., and Tilcock, C. P. (1985) in *Phospholipids and Cellular Regulation* (Kuo, J. F., ed) Vol. 1, pp. 1–59, CRC Press, Inc., Boca Raton, FL
55. Muñoz-Pinedo, C., Guio-Carrion, A., Goldstein, J. C., Fitzgerald, P., Newmeyer, D. D., and Green, D. R. (2006) *Proc. Natl. Acad. Sci. U. S. A.* **103,** 11573–11578
56. Garcia-Saez, A. J., Chiantia, S., Salgado, J., and Schwille, P. (2007) *Biophys. J.* **93,** 103–112
57. Chanturiya, A. N., Basañez, G., Schubert, U., Henklein, P., Yewdell, J. W., and Zimmerberg, J. (2004) *J. Virol.* **78,** 6304–6312
58. Basañez, G. (2002) *Cell. Mol. Life Sci.* **59,** 1478–1490
59. Gong, X. M., Choi, J., Franzin, C. M., Zhai, D., Reed, J. C., and Marassi, F. M. (2004) *J. Biol. Chem.* **279,** 28954–28960
60. Huang, H. W., Chen, F. Y., and Lee, M. T. (2004) *Phys. Rev. Lett.* **92,** 198304
61. Basañez, G., Shinnar, A. E., and Zimmerberg, J. (2002) *FEBS Lett.* **532,** 115–120
62. Leontiadou, H., Mark, A. E., and Marrink, S. J. (2006) *J. Am. Chem. Soc.* **128,** 12156–12161
63. Hadders, M. A., Berringer, D. X., and Gros, P. (2007) *Science* **317,** 1552–1554

BIM and tBID Are Not Mechanistically Equivalent When Assisting BAX to Permeabilize Bilayer Membranes

Oihana Terrones, Aitor Etxebarria, Ane Landajuela, Olatz Landeta, Bruno Antonsson and Gorka Basañez

J. Biol. Chem. 2008, 283:7790-7803.
doi: 10.1074/jbc.M708814200 originally published online January 14, 2008
